LASER INTERFEROMETER GRAVITATIONAL WAVE OBSERVATORY
- LIGO -
CALIFORNIA INSTITUTE OF TECHNOLOGY
MASSACHUSETTS INSTITUTE OF TECHNOLOGY

Technical Note **LIGO-T1700223—v1** 2017/09/22

Inferring the Astrophysical Population of Black Hole Binaries

LIGO SURF Final Report

Osase Omoruyi, Yale University
Mentor: Alan Weinstein, California Institue of Technology

California Institute of Technology
LIGO Project, MS 18-34
Pasadena, CA 91125
Phone (626) 395-2129
Fax (626) 304-9834
E-mail: info@ligo.caltech.edu

Massachusetts Institute of Technology
LIGO Project, Room NW22-295
Cambridge, MA 02139
Phone (617) 253-4824
Fax (617) 253-7014
E-mail: info@ligo.mit.edu

LIGO Hanford Observatory
Route 10, Mile Marker 2
Richland, WA 99352
Phone (509) 372-8106
Fax (509) 372-8137
E-mail: info@ligo.caltech.edu

LIGO Livingston Observatory
19100 LIGO Lane
Livingston, LA 70754
Phone (225) 686-3100
Fax (225) 686-7189
E-mail: info@ligo.caltech.edu

http://www.ligo.caltech.edu/

1 Abstract

LIGOs gravitational wave detections have not only established the existence of black hole binaries, but also confirmed the presence of stellar mass black holes larger than 20 solar masses. Our project aims to study these binaries and their mass distribution throughout space. Currently, LIGO has made 4 detections of binary black hole mergers. However, this sample is too small to draw significant conclusions about the mass distribution. To circumvent this problem, our project looks towards the future. Within the next 10 years, LIGO expects the number detections to rise significantly. With these future detections in mind, our project utilizes simulated data to generate a large population of black hole binaries. From our general astrophysical knowledge about black holes and nature, we expect the underlying population to fall like a power-law in the mass of the larger black hole, $M^{-\alpha}$, in which α is the power-law index. With the large sample of events our simulations provide, we aim to constrain the value of the power-law index more precisely and accurately. By doing so, we will be able to constrain the black hole mass distribution and use that information to make inferences about the formation and evolution of black hole binaries.

2 Background and Motivation: Exploring Binary Black Hole Formation and Evolution From the Mass Distribution

On September 14, 2015, LIGO confirmed the existence of black hole binaries by detecting the gravitational waves emitted from the merger of the black holes within the binary [1]. This discovery was not only remarkable because it confirmed Einstein's prediction of gravitational waves within his theory of general relativity, but because it revealed a population of black hole binaries– particularly black hole binaries larger than 20 solar masses. Before LIGO's detections, astronomer's had primarily relied on x-ray studies to find black holes. This method, while effective, did not detect any black holes above 20 solar masses. As a result, LIGO's 3 detections, extend the range of the known mass distribution of black holes [**?**].

This mass distribution is important to astronomers because it can tell us how black hole binaries form and evolve over time [2]. Currently, there are two scenarios that dominate the potential origin of black hole binaries: dynamical capture and isolated binary evolution. In dynamical capture, one black hole captures another black hole from another system into an orbit. You can tell the black holes did not evolve together originally because their spins are misaligned. In isolated binary evolution, the black hole binary is developed from a previous star-star binary. Both stars evolved into black holes, meaning that each star withstood being blown away by each other's supernova.

The mass distribution is one method by which astronomers may confirm which formation scenario dominates binary black hole systems.

In the future, as the network of ground-based GW detectors grows, LIGO expects to have increased detector sensitivity and more observing runs [3]. As a result of this expansion and overall improvement, we expect there to be on the order of tens, hundreds, and eventually thousands of gravitational wave events. This will allow us to form a population of events that we can be able to draw significant conclusions about the mass distribution. By constraining the mass distribution, we will be gaining valuable information on how black hole binaries formed and evolved over time.

However, before we project into the future, we must focus on the present and prepare for the data to come. With 4 known events, we have begun to form a small population of binary black hole (BBH) mergers. This number, however, is too small to make substantial inferences about the nature of BBH systems. Because we will not have a large sample of events for decades to come, we must devise methods to make inferences about BBHs from the data and knowledge we have available now. This is where our research becomes relevant.

The overarching goal of our project is to project into the future where LIGO has multiple events by making use of simulated data. To do this, we aim to create a simulated mass distribution of black hole binaries to the farthest distances of the observable universe and recover that mass distribution from the simulated events we would expect LIGO to detect. By doing this, we will be able to determine the actual mass distribution of black hole binaries when LIGO has more events in the future.

3 Method and Results

3.1 Simulating Black Hole Binaries

We created simulations of black hole binaries by taking into account parameters that described the binary and the parameters that described the black holes within the binary. These parameters are listed in Tables 1 and 2 below. We used our astrophysical knowledge of black holes to create models that would describe the distribution of BBH based on each parameter.

3.1.1 Parameters Describing The Binary

Parameter	Symbol	BBH Distribution
Right Ascension	α	Uniform
Declination	δ	Uniform in cosδ
Luminosity Distance	d_L	Volumetric
Orbital Inclination	ι	Uniform in cos ι
Time of Coalescence	t_c	Uniform
Phase of Coalescence	φ_c	Uniform in [0,2]pi

Table 1: Summary of Parameters Describing The Binary

Sky Location: Right Ascension and Declination

According to the cosmological principal [4], the large scale spatial distribution of matter in the universe is homogeneous. Therefore, the universe should look the same when viewed on a large enough scale, and there should be no observable pattern anywhere. Following the cosmological principal, we expect to see a random distribution of BBH across the sky because BBH are not concentrated in one single area of the universe. To best see the distribution of BBH according to sky location we used a Mollweide Projection map, as shown in Figure 1.

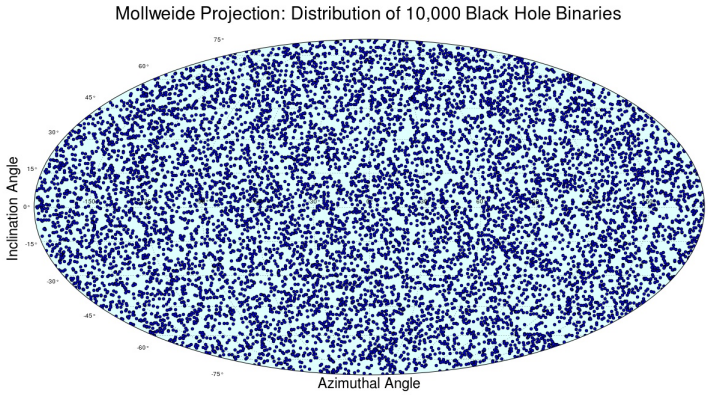

Figure 1: The distribution of Binary Black Holes in a Mollweide Projection. As expected, the simulation of 10,000 BBHs are randomly distributed throughout the sky.

Luminosity Distance

To simulate the distribution of binary black holes according to luminosity distance, we may assume a population of BBHs lie within a given radial distance. Given the cosmological principal and the radial distribution of BBHs, we expect the distribution of BBHs to increase exponentially as we observe further from Earth, as shown in Figure 2. This is because as the distance increases, the volume of BBH increases as a power law due to the r^3 factor in the volume equation.

$$Equation..1 : V = \frac{4}{3}\pi r^3$$

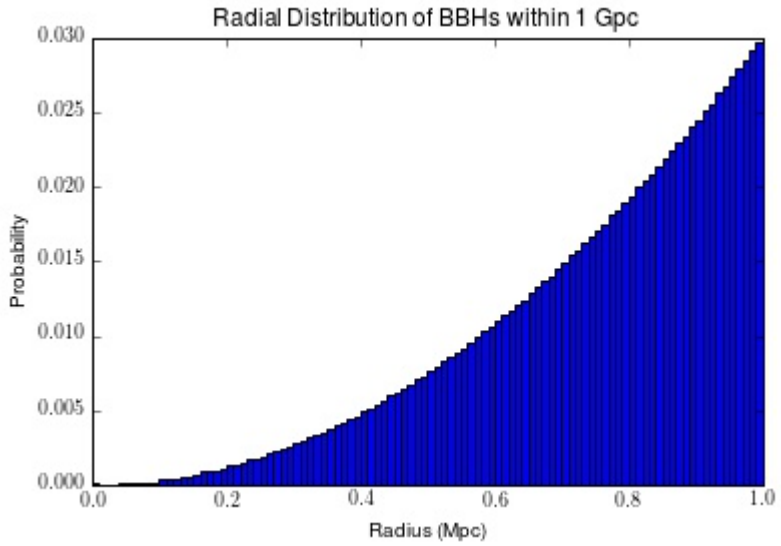

Figure 2: The radial distribution of Binary Black Holes within a luminosity distance of 1 Gpc. We expect the distribution of BBH to increase exponentially as we observe further from Earth.

Orbital Inclination

Binary black holes do not always directly face our detectors. Instead, many BBH systems are inclined at a certain angle with respect to the detectors. The inclination angle of the system directly effects the magnitude of the gravitational wave strain detected. Gravitational Waves from a BBH system with a face-on orbital plane will have larger amplitude than from a system of an edge-on orbital plane; thus, one needs to know both the amplitude and the orbital inclination of the system to infer the luminosity distance of a BBH merger. We expect the inclination angle of the system to range anywhere between 0 and π and be uniform in $cos(\iota)$.

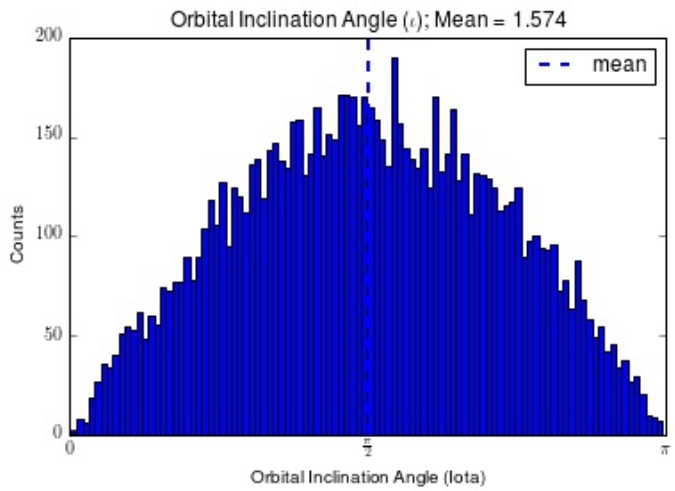

Figure 3: Orbital Inclination Angle (ι). We can see the inclination angle of the system ranges randomly between 0 and π.

Time of Coalescence

BBH mergers may occur at any given time during an observation run. However, the detectors are not always on-line to detect the merger. The Livingston detector is on approximately 61% of the observing run and the Hanford detector 56%. In order to confirm a BBH merger, LIGO requires both detectors to be on-line to check the time consistency as the gravitational waves travel from one detector to another. Gravitational waves travel near the speed of light. Therefore, the difference in time of detection between the Livingston and Hanford detectors serves as an additional means of confirmation. Figure 4 shows the probability of one detector, both detectors or neither detector being on during the observing run.

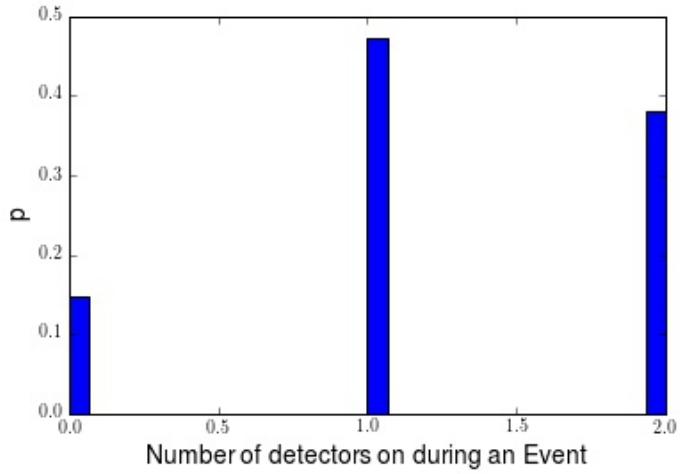

Figure 4: Number of detectors on during an observing run. We expect both detectors to be on at the same time for about 30% of the run.

Phase of Coalescence

Each black hole within the BBH system orbits around the other. As time passes and they begin to orbit each other faster and faster, they emit more and more energy and get closer and closer together. This is known as the phase of coalescence. The phase of coalescence of BBH systems determines whether the gravitational waveform emitted is cosine-like, sine-like, or in-between, relative to the time of coalescence. We expect BBH systems to have random φ_c between 0 and 2π, as shown in Figure 5, because the phase at coalescence is observer-dependent, and there is nothing special about us as observers.

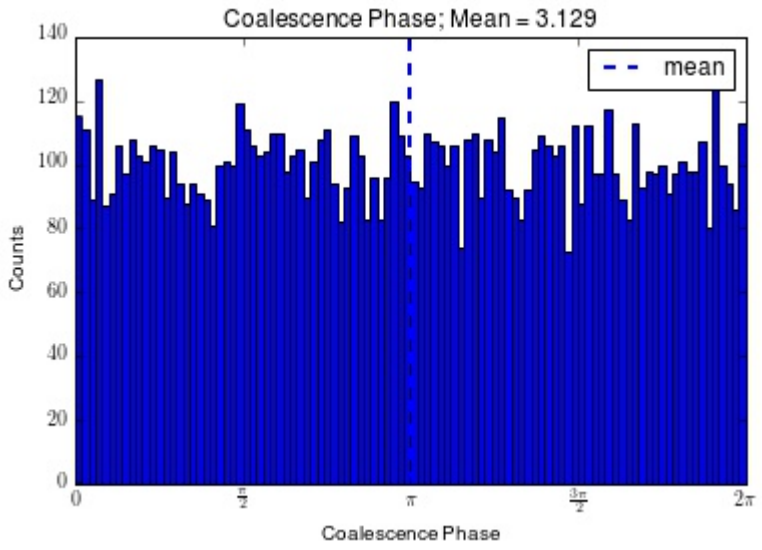

Figure 5: Phase of Coalescence. As see, we expect the distribution of phases for BBH to range from 0 to 2π.

3.1.2 Parameters Describing The Black Holes Within the Binary

Parameter	Symbol	BBH Distribution
Total Mass	M	Power Law
Symmetric Mass Ratio	η (m_1, m_2)	Gaussian
Spin Magnitude	a_1, a_2	Gaussian
Spin Azimuthal Angle	ϕ_{a1}, ϕ_{a2}	Uniform in $[0, 2\pi]$
Spin Polar Angle	μ_{a1}, μ_{a2}	Uniform in $\cos\mu$

Table 2: Summary of Parameters Describing The Black Holes Within the Binary

Total Mass

To simulate the distribution of BBH masses, we used the Initial Mass Function for massive stars postulated by Edwin Salpeter shown in Equation 2 [5].

$$Equation..2 : \xi(M)\Delta M = \xi_0 (M/M_\odot)^{-2.35} (\Delta/M_\odot)$$

$$N = \int_{M_l}^{M_u} \xi_0 \Big[(M/M_{sun})^{-2.35} \Big] dM$$

According to the Initial Mass Function, there are more low mass stars than high mass stars because low mass stars live longer and therefore contribute to most of the stellar mass in a system. Since black holes are formed from the collapse of stars, we may also apply the IMF to the distribution of BBH. In our simulations, we chose to generate BBH masses between 10 and $100M_{\odot}$ because higher mass systems produce louder (higher amplitude) GWs, so we can detect them over a larger volume. As a result of using the IMF, we expected the majority of our simulated BBHs to lie between 10-30$M_{\odot}$, as shown in Figure 6.

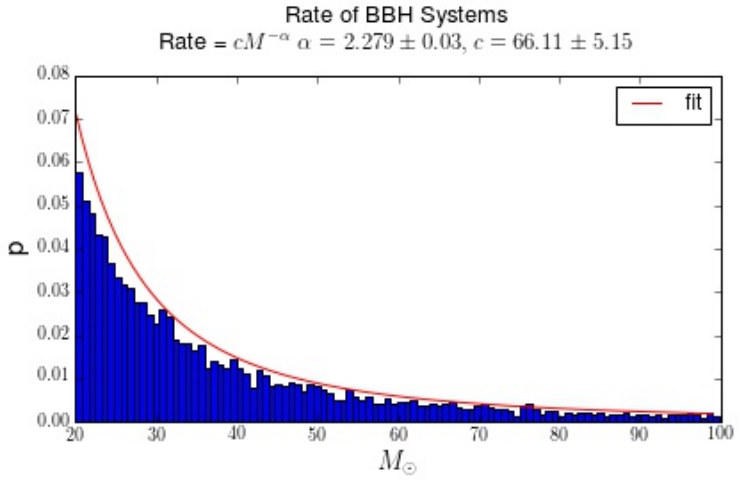

Figure 6: Distribution of Total Mass in BBHs. As seen, in the distribution of BBH in the range from 10-100$M_{\odot}$,the majority of the BBH are between 10-30$M_{\odot}$.

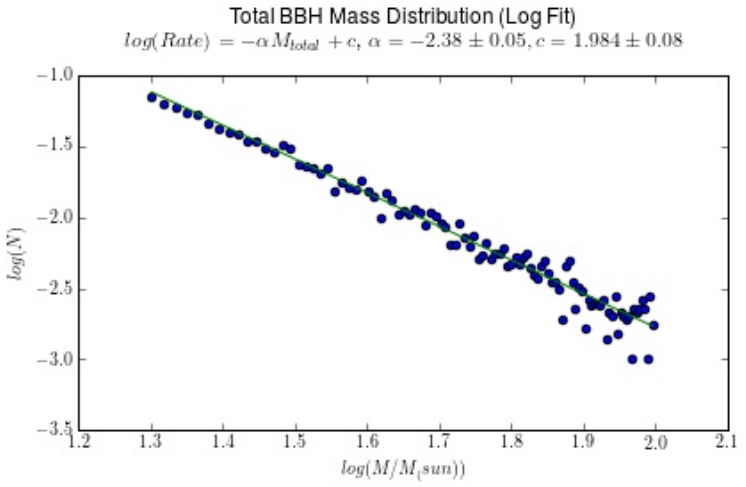

Figure 7: Log Fit of Mass Distribution. The distribution is linear, as expected from a log fit of a power law.

Symmetric Mass Ratio

Each black hole within the binary has its own individual mass. We postulate that the formation mechanisms dominating in nature favor roughly equally distributed mass, so we expect the mass ratio, q, between the two black holes in the binary to be close to 1.

To simulate the symmetric mass ratio parameter eta, η, we decided to extend q's range from 1 to 10. η allows us to characterize the BBH system.

$$Equation..3 : \eta = \frac{q}{(1+q^2)} = \frac{(M_1 * M_2)}{(M_1 + M_2)^2}$$

We know the total mass of the binary.

$$Equation..4 : M_{total} = M_1 + M_2$$

Using these two equations, we can solve for M_1 and M_2 in terms of total mass and eta.

$$Equation..5a : M_1 = \frac{M_{total} + \sqrt[2]{(M_{total}^2 * (1 - 4 * \eta))}}{2}$$

$$Equation..5b : M_2 = \frac{M_{total} - \sqrt[2]{(M_{total}^2 * (1 - 4 * \eta))}}{2}$$

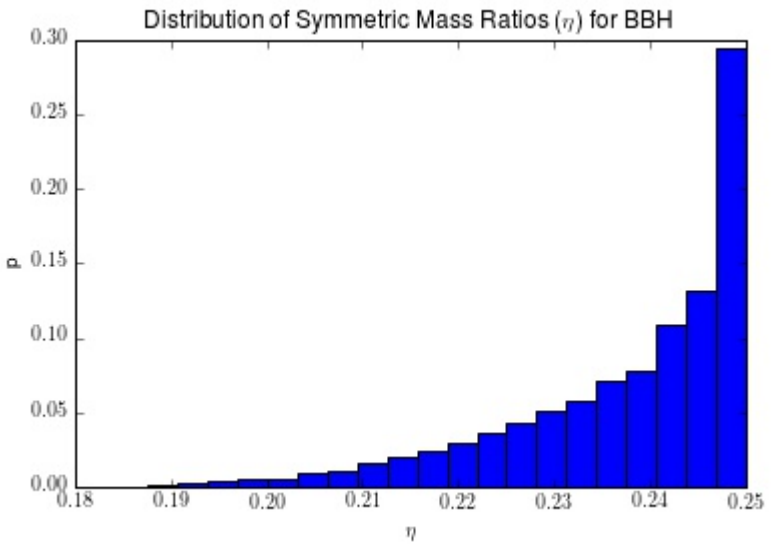

Figure 8: Distribution of Symmetric Mass Ratios (η) for BBH. We simulated it as a half-Gaussian with mean of 0.25 and width of 0.05, with some cutoff. When η is 0.25, q is 1. Seeing how the mass is distributed in the IMF, we should expect η to be near 0.25.

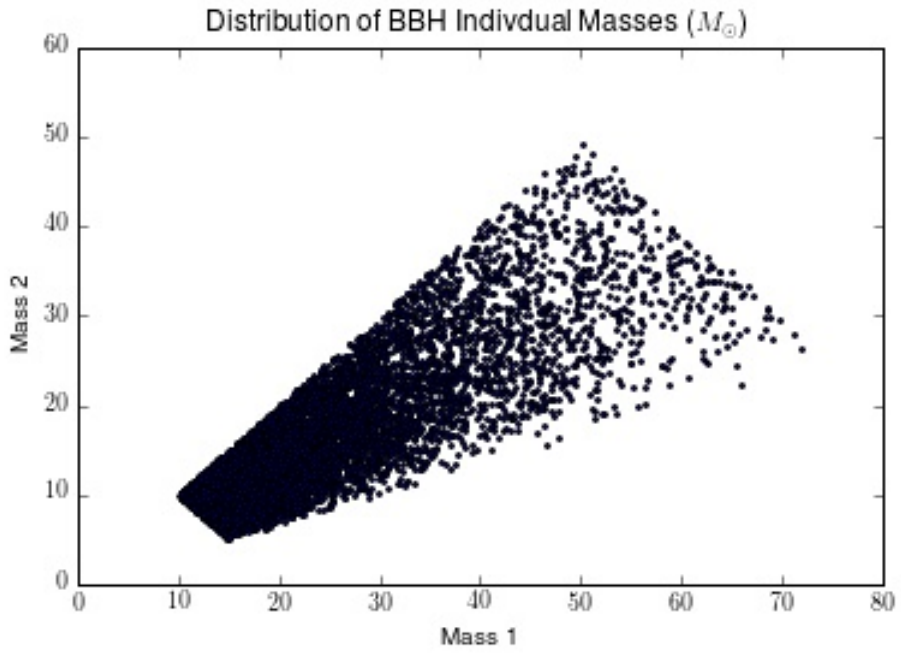

Figure 9: Distribution of BBH Individual Masses. The average value for q appears to be less than 2, which is expected due to the distribution of total mass according to the IMF.

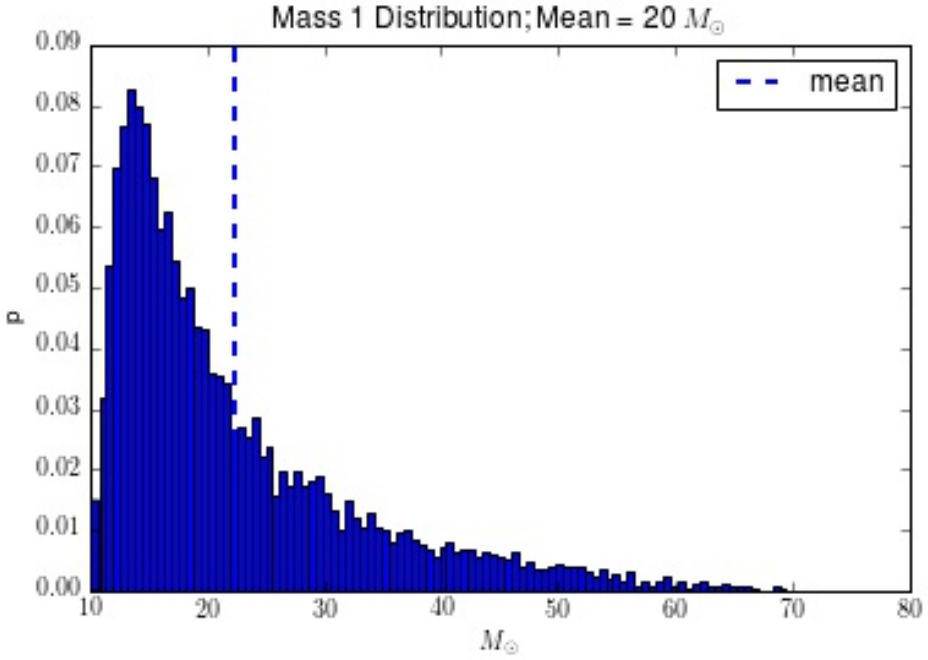

Figure 10: Mass 1 Distribution. The average mass is 21 $m_\odot$.

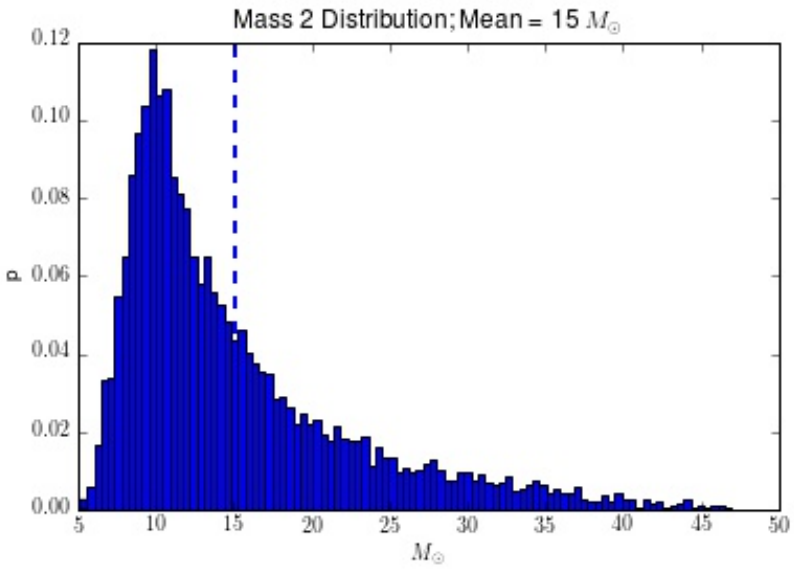

Figure 11: Mass 2 Distribution. The average mass is 11 $m_\odot$.

Spin Magnitude

The spin of a black hole is a dimensionless parameter that describes the ratio of black hole's observed angular momentum to the maximal angular momentum predicted by the Kerr solution [6]. We assumed the spins of BBH are distributed in a Gaussian distribution of 0.7 mean and 0.1 std.

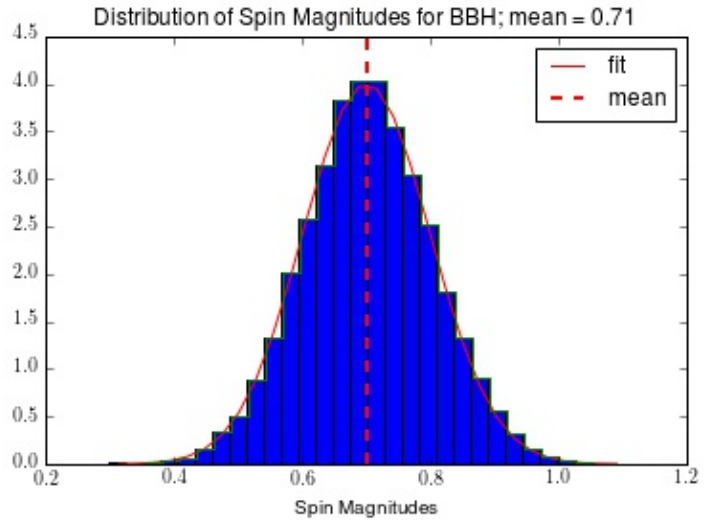

Figure 12: Distribution of Spin Magnitudes for BBH. The spins of BBH are distributed in a Gaussian distribution of 0.7 mean and 0.1 std. Values larger than 1 were not accepted, as the spin is a ratio of angular momentum between 0 and 1.

Spin Azimuthal and Polar Angles

If the spin of each black hole within the binary points in the same direction as the total angular momentum of the system, the magnitude of the spins will not be influenced by the inclination of the black holes. More generally, the black hole will spin at certain angles away from the total angular momentum of the system. These angles are known as the polar and azimuthal angles of the spin. We expect the polar angle of the spin to range from 0 to π and the azimuthal angle of the spin to range from 0 to 2π.

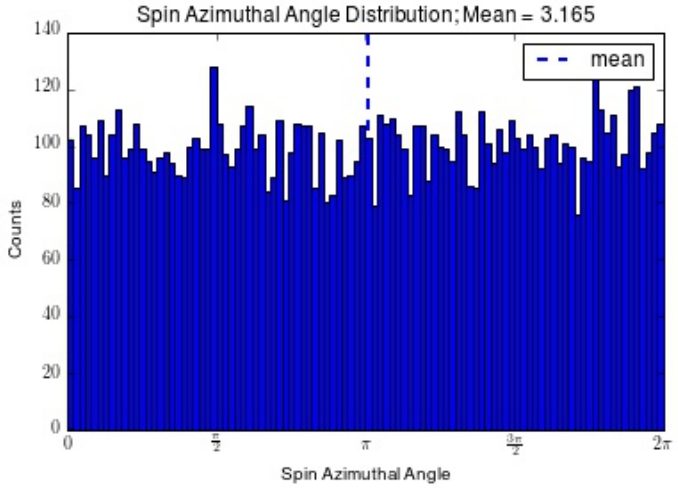

Figure 13: Spin Azimuthal Angle Distribution. We can see the azimuthal angle of the spin ranges from 0 to 2π.

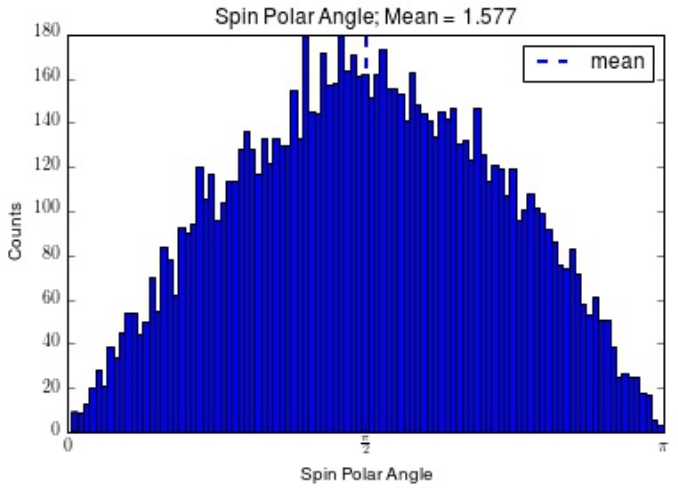

Figure 14: Spin Polar Angle Distribution. We can see the polar angle of the spin ranges from 0 to π.

3.2 Modeling and Refining the Natural Rate Density of Black Hole Binaries

In our simulations of black hole binaries, we assumed the mass distribution of these systems fell like a power law of mass raised to the negative power of alpha, the power-law index, in which the power-law index is defined as 2.35 by Edwin Salpeter's Initial Mass Function[5].

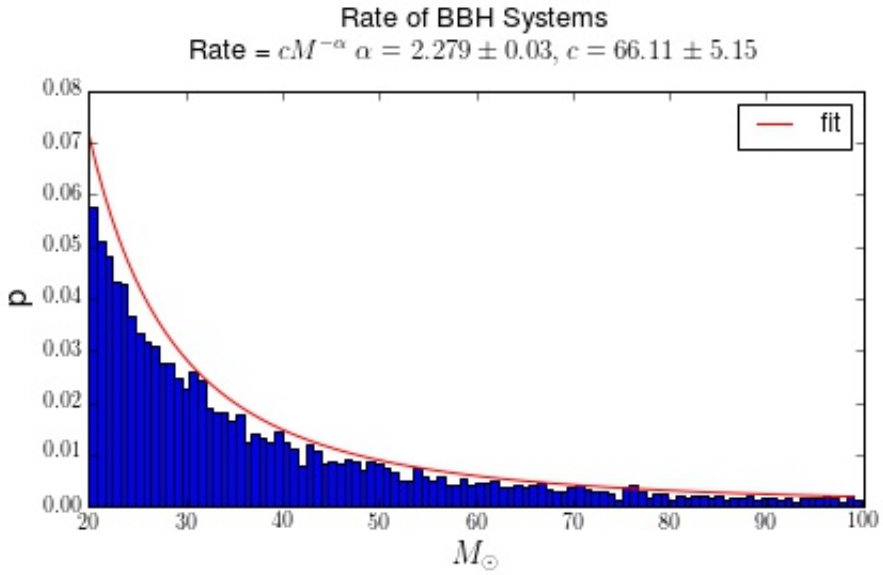

Figure 15: Total Mass Distribution of BBH Systems. The mass is distributed by the power law $M^{-2.35}$

The natural rate density of black hole binaries is the number of binaries of given mass per unit volume in a given time frame. It is dominated by the power-law index. The goal of our project is to recover our chosen power-law index from the number of detectable simulated events. By successfully recovering our rate from simulated events, future LIGO may also use our work to recover the rate density of binary black holes when they have more events. Recovering the rate density will allow us to understand how the mass of binary black holes is distributed, which in turn will allow us to infer how black hole binaries have formed and evolved over time.

To create simulated observations of the natural rate density of black hole binaries, we must find a way to relate the number of detectable observed events to the natural rate density. We can do this using Equation 6, in which N(m) is the observed number of black hole binaries of given mass, R(m) is the natural rate density, V(m) is the volume in which the black hole binaries lie and T is a given time-frame.

$$Equation...6 : N(m) = R(m)V(m)T$$

To find $N(m)$, we must recognize that not all of our simulated events are detectable by LIGO. We consider events to be detectable if they have a signal-to-noise ratio (SNR) greater than 8 in both the Hanford and Livingston detectors. To calculate the SNR, we generated gravitational waveforms from our simulated parameters of black hole binaries. Using these

waveforms, we created plots of the event in the time domain and plotted the frequency of the event against a smooth model of LIGO's Amplitude Spectral Density (ASD) curve for visualization purposes.

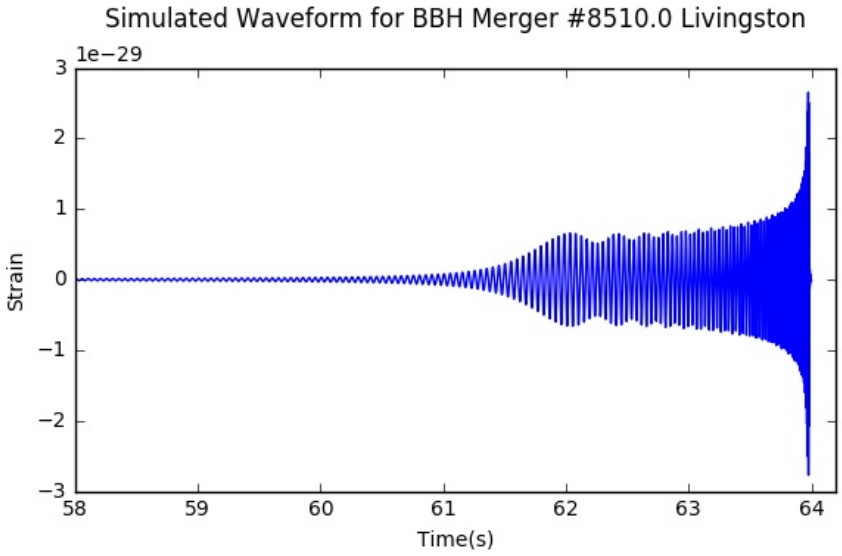

Figure 16: Sample Simulated Gravitational Waveform in the Livingston Detector.

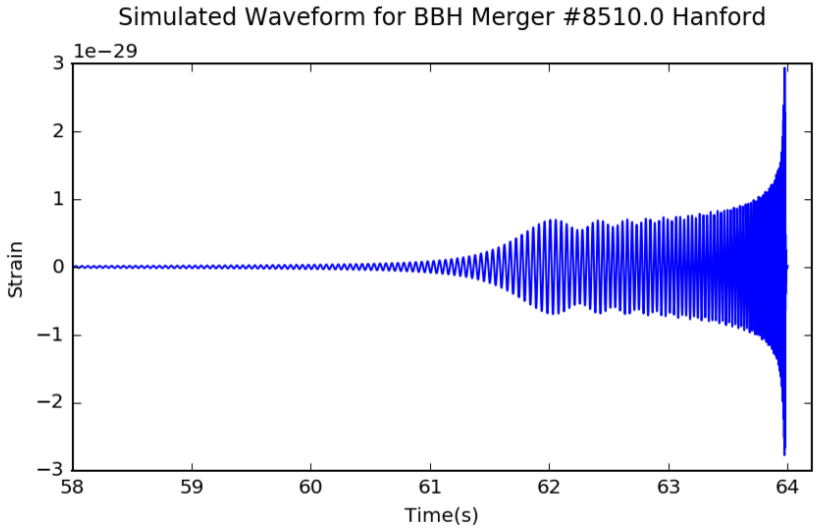

Parameters: $M_1 = 14.2968550704\ M_\odot$, $M_2 = 23.5374637484\ M_\odot$, $S_1 = 0.773573778241$, $S_2 = 0.84603689721$, $RA = 166.035867307$, $Dec = -21.1142384009$, $Phase = 3.23287426483$, $Distance = 0.425983879719\ Gpc$

Figure 17: Sample Simulated Gravitational Waveform in the Hanford Detector.

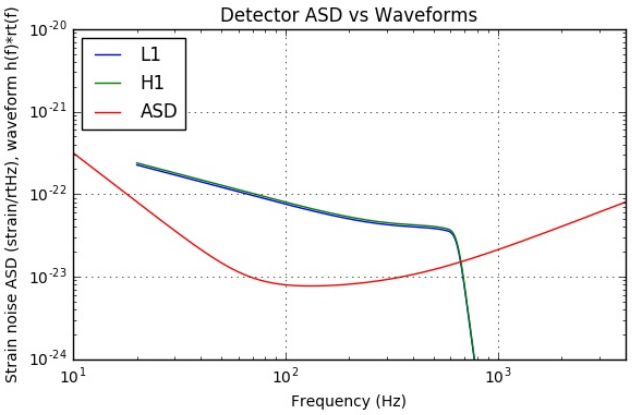

Figure 18: ASD curve of Detectors at Hanford and Livingston vs the Frequency of the Sample Simulated Gravitational Waveforms.

After visualizing the waveforms, we calculated the SNR by making use of optimal matched filtering. The matched filter is the optimal filter for detecting a signal in stationary Gaussian noise ($S_n(f)$). In this process, we match the signal's data($\bar{s}(f)$) with a filter template ($\bar{h}_t(f)$) and calculate the output using Equation 7. [7]

$$Equation..7 : z(t) = 4Re \int_0^\infty \frac{\tilde{s}^*(f)\bar{h}_t(f)}{S_n(f)} e^{2\pi i f t} df$$

The use of the FFT allows us to search for all possible arrival times of the signal. The peak of the magnitude $|z(t)|$ of the matched filter output tells us the SNR of the signal.

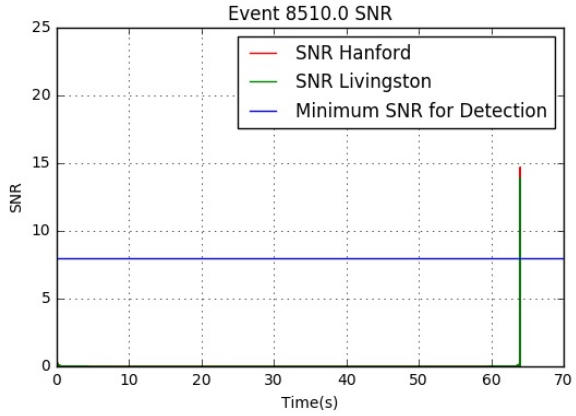

Figure 19: SNR at Hanford vs. SNR at Livingston. The SNR at Hanford is 14.7. The SNR at Livingston is 13.9.

We generated a total of 100,000 gravitational waveforms and calculated the SNR of each of our simulated events. We then conducted an acceptance-rejection process that accepted events with $SNR > 8$ in both detectors and rejected all events that did not meet that

requirement. Initially, we found that less than 10% of our events met these requirements. To make our acceptance-rejection process more efficient, we decided to simulate each event out to its optimal horizon distance only. For a single detector, the optimal horizon distance is defined as the distance at which an optimally-oriented, overhead source may be detected with a SNR $\rho(D_{horizon}) = 8$, where [8]

$$\rho = \sqrt[2]{4 \int_0^{f_{max}} \frac{|h(f)|^2}{S_n(F)} df}$$

f_{max} is the Nyquist frequency, which is half of the sample rate. Advanced LIGO samples at 16384 Hz, so $f_max = 8192$ Hz [9]. However, we sampled at 4096 Hz ($f_max = 2018$ Hz) since that's the frequency needed for higher-mass BBH mergers.

By simulating out to the optimal horizon distance for each event, we increased the number of accepted events to about 20,000, increasing our efficiency to 20%.

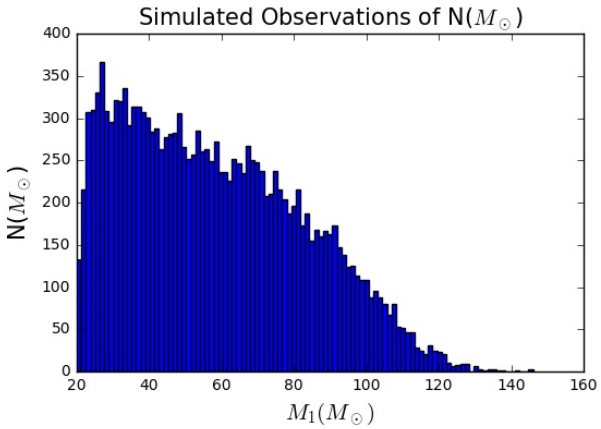

Figure 20: Observed events with $SNR > 8$ in both Hanford and Livingston detectors

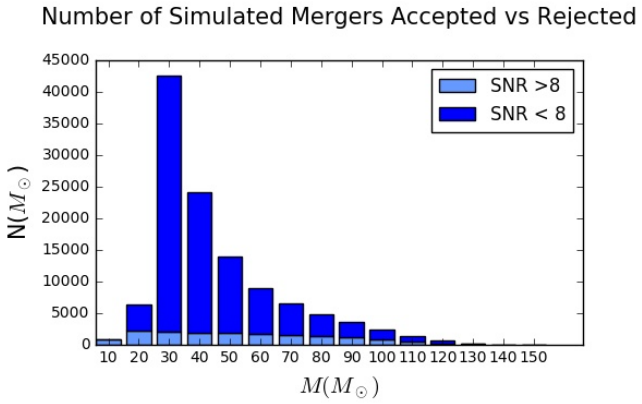

Figure 21: Events with $SNR > 8$ vs events with $SNR < 8$.

To calculate the volume of the observed events as a function of mass, we related the observed volume to the volume of the universe using the fraction of detectable events. We chose the radius of the universe to be 10 Gpc. This step allows us to account for the fact that we only generated BBH randomly out to their horizon distance.

$$V_u = \frac{4\pi d_u^3}{3}, d_u = 10Gpc$$

$$V_o = f_{SNR>8} * V_u$$

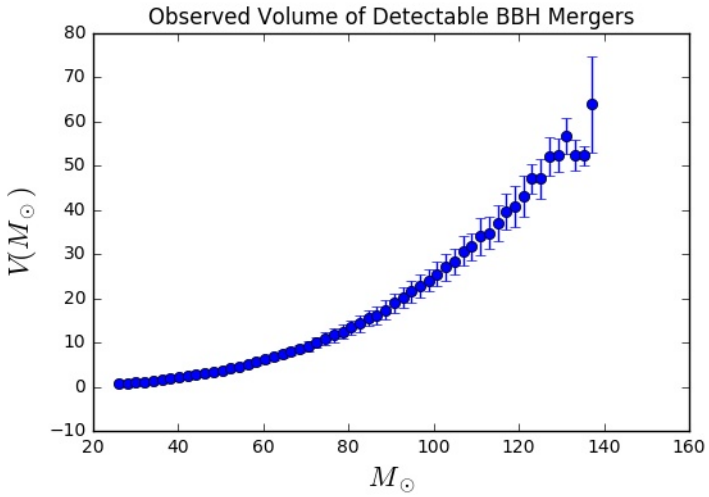

Figure 22: Observed volume of detectable events.

Now that we have determined the number of observable events, their volume and time, we can calculate the rate density. We can relate the number of BBH in our simulated universe to the Rate using:

$$R(m_{total}) = \frac{N_o(m_{total})}{V_o(m_{total})T}$$

With the rate, we now devised a method to constrain the alpha parameter of the rate function. To do this, we look back to the IMF. From the IMF, we know that the Rate Density is dominated by the power-law index α.

$$R(m_{total}) = C m_{total}^{-\alpha}$$

$$R_{true} = \int dm_{total} R(m_{total}) = C \int_{m_{min}}^{m_{max}} m_{total}^{-\alpha} dm_{total}$$

Normalization factor: $I_\alpha = \int_{m_{min}}^{m_{max}} m_{total}^{-\alpha} dm_{total}$

$$R(m_{total}) = \frac{R}{I_\alpha} m_{total}^{-\alpha}, \frac{R}{I_\alpha} = C$$

Using curve fit, we determined the rate and a rough estimate for α.

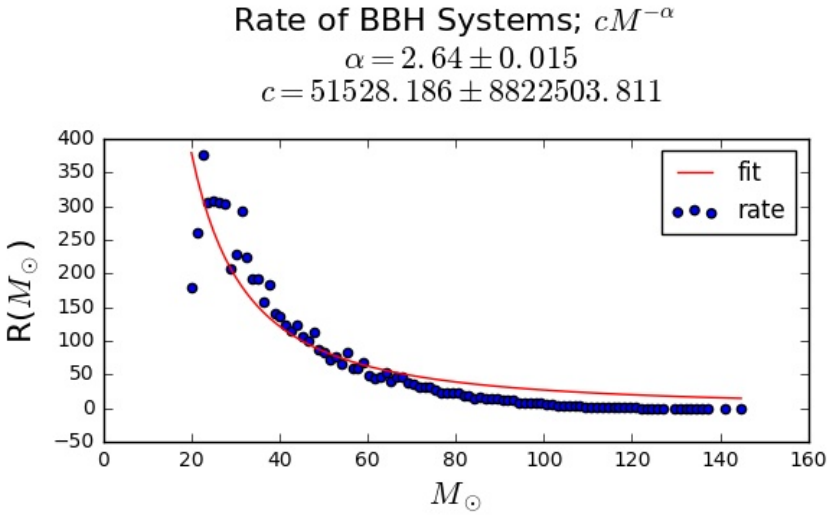

Figure 23: Rate of Binary Black Holes. $\alpha = -2.688 \pm 0.015$.

3.3 Using Bayesian Parameter Estimation to Constrain α

To analyze how well we recovered α, we used Bayesian parameter estimation by fitting the Rate to a linear model.

$$\log(Rate) = -\alpha \log(M) + \log(c)$$

$$y = mx + b$$

with f as the error on the $\log(Rate)$. According to Bayes' Theorem

$$p(H|E) = \frac{p(H) * P(E|H)}{P(E)}$$

where $p(H|E)$ is the posterior probability of hypothesis "H" given the evidence, P(H) is the prior probability, p(E) is the evidence and $P(E|H)$ is the likelihood of the evidence if the hypothesis "H" is true.

Prior function: $p(m, b, f)$

Priors: p(m) =

$$p(m) = \begin{cases} 1/5, if -5 < m < 0 \\ 0, otherwise \end{cases}$$

$$p(b) = \begin{cases} 1/20, if 0 < b < 20 \\ 0, otherwise \end{cases}$$

$$p(lnf) = \begin{cases} 1/10, if -5 < lnf < 5 \\ 0, otherwise \end{cases}$$

Likelihood function: $p(y|x, \sigma, m, b, f)$

In our case, we take the log-likelihood because it is more convenient to work with. Log Likelihood function: $\ln p(y|x, \sigma, m, b, f)$

$$\ln p(y|x, \sigma, m, b, f) = -\frac{1}{2} \sum_n \left[\frac{(y_n - mx_n - b)^2}{s_n^2} + ln(2\pi s_n^2) \right]$$

where

$$s_n^2 = \sigma_n^2 + f^2(mx_n + b)^2$$

Posterior probability function:

$$p(m, b, f|x, y, \sigma \approx p(m, b, f)p(y|x, \sigma, m, b, f)$$

Using Bayesian parameter estimation, we created corner plots of the posterior probability distribution of α.

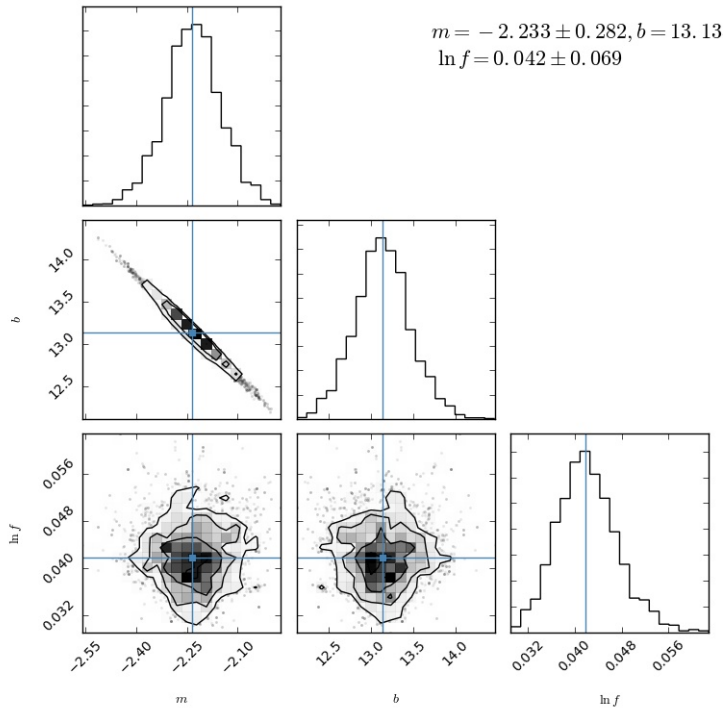

Figure 24: Corner plot showing the Posterior probability Distribution of α, β and $\ln f$.

3.4 Recovering the Natural Rate Density from Realistic Near-Future Event Numbers

Initially, we simulated 100,000 detectable black hole binaries. However, LIGO will most likely not detect this amount of black hole binaries within the next one hundred years. To make this project more relevant to LIGO's near-future goals, we scaled the number of events down to a range of 10 to 1000. This allowed us to see how well we could recover the natural rate density given a limited number of events.

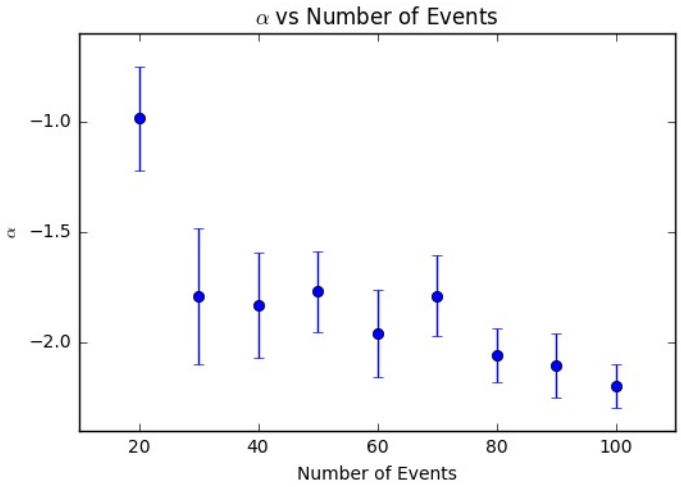

Figure 25: α vs the number of events.

As shown in Figure 25, the error on α decreases as the number of events increases. Therefore, as LIGO detects more events within the next 10-20 years, we will be able to constrain the value of α more precisely and accurately.

4 Conclusions and Future-Work

The mass distribution of BBH can be a very useful tool in understanding how binary black hole systems formed and evolved over time. Within the next 10-20 years, LIGO expects to detect on the order of tens of events, which will provide a population large enough to draw substantial conclusions about the mass distribution of BBH, as shown in Figure 25.

By simulating our own binary black hole mergers and recovering the mass distribution we originally inputed from the observed simulated events within error, we have shown that it will be possible to accurately recover the mass distribution of binary black holes in the future. If the mass is distributed as power law in the total mass of the BBH system, our method of modeling the rate density will be useful in recovering the mass distribution.

It is important to note that a more thorough version of this project would entail calculating the rate density for all kinds of models for the mass distribution. Having a breadth of models would allow us to explore other scenarios in which alpha is another value other than -2.35,

the mass is not distributed in the total mass of the system or the rate density is not a power law at all. Fortunately, more work can and is being done to test multiple models of the mass distribution of binary black holes.

5 Acknowledgements

We thank the National Science Foundation and the Carl Albert Rouse Fellowship for sponsoring and supporting our research in the 2017 LIGO SURF program at Caltech. Our research would not have been possible without their support. We also thank all researchers in the LIGO Scientific collaboration, SURF students included, who helped us along.

References

[1] B. P. Abbott, R. Abbott, T. D. Abbott, M. R. Abernathy, F. Acernese, K. Ackley, C. Adams, T. Adams, P. Addesso, R. X. Adhikari, and et al. Observation of Gravitational Waves from a Binary Black Hole Merger. *Phys. Rev. Lett.* , 116(6):061102, February 2016.

[2] B. P. Abbott, R. Abbott, T. D. Abbott, M. R. Abernathy, F. Acernese, K. Ackley, C. Adams, T. Adams, P. Addesso, R. X. Adhikari, and et al. Astrophysical Implications of the Binary Black-hole Merger GW150914. *Astroph. J. Lett.* , 818:L22, February 2016.

[3] S. Vitale and M. Evans. Parameter estimation for binary black holes with networks of third-generation gravitational-wave detectors. *Phys. Rev. Lett.* , 95(6):064052, March 2017.

[4] I. Newton. *Philosophiae naturalis principia mathematica*. J. Societatis Regiae ac Typis J. Streater, 1687.

[5] E. E. Salpeter. The Luminosity Function and Stellar Evolution. *Astroph. J. Lett.* , 121:161, January 1955.

[6] M. Visser. The Kerr spacetime: A brief introduction. *ArXiv e-prints*, June 2007.

[7] B. Allen, W. G. Anderson, P. R. Brady, D. A. Brown, and J. D. E. Creighton. FINDCHIRP: An algorithm for detection of gravitational waves from inspiraling compact binaries. *Phys. Rev. Lett.* , 85(12):122006, June 2012.

[8] J. Abadie, B. P. Abbott, R. Abbott, M. Abernathy, T. Accadia, F. Acernese, C. Adams, R. Adhikari, P. Ajith, B. Allen, and et al. TOPICAL REVIEW: Predictions for the rates of compact binary coalescences observable by ground-based gravitational-wave detectors. *Classical and Quantum Gravity*, 27(17):173001, September 2010.

[9] LIGO Scientific Collaboration, J. Aasi, B. P. Abbott, R. Abbott, T. Abbott, M. R. Abernathy, K. Ackley, C. Adams, T. Adams, P. Addesso, and et al. Advanced LIGO. *Classical and Quantum Gravity*, 32(7):074001, April 2015.